

Adaptive Hydrogen-Bonding Strategy Driven 0D Manganese-Based Metal Halides with Multifunctional Fluorescent Applications

Jiamin Liu,^{a, b} Yuntao Ruan,^{a, b} Qiaoqi Qin,^{a, b} Yong Shen,^a Zhengliang Wang,^c Daibin Kuang,^a and Long Jiang *^b

a. Key Laboratory of Bioinorganic and Synthetic Chemistry of Ministry of Education, Guangdong Basic Research Center of Excellence for Functional Molecular Engineering, School of Chemistry, Institute of Green Chemistry and Molecular Engineering, Sun Yat-sen University, Guangzhou 510275, China.

b. Instrumental Analysis and Research Center, Sun Yat-sen University, Guangzhou, 510275, P. R. China.

c. Key Laboratory of Advanced Synthetic Chemistry (Yunnan Minzu University) of State Ethnic Affairs Commission, Key Laboratory of Green-chemistry Materials in University of Yunnan Province, School of Chemistry & Environment, Yunnan Minzu University, Kunming, 650500, P. R. China.

Contents

Part 1. Supporting tables.....	3
Part 2. Supporting figures.....	6

1. Supporting tables

Table S1 Crystallographic data and structural refinements for 1 and 2.

Parameters	1	2
Chemical formula	C ₁₆ H ₃₂ Br ₄ MnN ₄	C ₁₆ H ₅₂ Br ₄ MnN ₄ O ₁₀
Formula weight	655.03	835.19
Temperature [K]	150.0	150.0
Crystal system	monoclinic	monoclinic
Space group (number)	P2 ₁ /c (14)	P2 ₁ /c (14)
<i>a</i> [Å]	10.9769(9)	9.2231(8)
<i>b</i> [Å]	16.9599(14)	14.0026(12)
<i>c</i> [Å]	12.4404(11)	12.7924(9)
α [$^\circ$]	90	90
β [$^\circ$]	90.029(3)	101.865(3)
γ [$^\circ$]	90	90
Volume [Å ³]	2316.0(3)	1616.8(2)
<i>Z</i>	4	2
ρ_{calc} [gcm ⁻³]	1.879	1.716
μ [mm ⁻¹]	8.591	6.461
<i>F</i> (000)	1284	842
Radiation	GaK _{α} ($\lambda = 1.34138 \text{ \AA}$)	GaK _{α} ($\lambda = 1.34138 \text{ \AA}$)
Reflections collected	21579	24109
Independent reflections	4937	3567
	$R_{\text{int}} = 0.0488$	$R_{\text{int}} = 0.0724$
	$R_{\text{sigma}} = 0.0429$	$R_{\text{sigma}} = 0.0528$
Completeness	97.5 %	99.8 %
Goodness-of-fit on F^2	1.050	1.060
Final <i>R</i> indexes	$R_1 = 0.0400$	$R_1 = 0.0426$
[$I \geq 2\sigma(I)$]	wR ₂ = 0.1147	wR ₂ = 0.0947
Final <i>R</i> indexes	$R_1 = 0.0400$	$R_1 = 0.0709$
[all data]	wR ₂ = 0.1168	wR ₂ = 0.1066
Largest peak/hole [eÅ ⁻³]	1.99/-0.58	0.62/-1.04
CCDC No.	2441615	2403071

^a $R_I = \Sigma ||F_o| - |F_c|| / \Sigma |F_o|$; wR₂ = $\{[\Sigma w(F_o^2 - F_c^2)^2] / \Sigma [w(F_o^2)^2]\}^{1/2}$.

Table S2 Hydrogen bonds for 1.

D-H···A	D-H/Å	H-A/Å	D-A/Å	D-H-A/°
C1-H1A···Br2 ¹	0.99	2.72	3.705(4)	176.2
C1-H1B···Br2 ²	0.99	2.77	3.720(4)	160.1
C2-H2A···Br1 ²	0.99	3.09	3.990(4)	151.3
C2-H2A···Br3 ²	0.99	3.10	3.794(4)	128.2
C3-H3A···Br2 ²	0.99	3.20	3.976(4)	136.2
C3-H3A···Br3 ³	0.99	3.36	3.958(4)	121.1
C3-H3B···Br1	0.99	3.06	3.948(4)	149.4
C5-H5A···Br1	0.99	2.91	3.764(4)	145.2
C5-H5B···Br1 ¹	0.99	2.85	3.648(4)	138.5
C6-H6A···Br1 ¹	0.99	2.99	3.744(5)	134.1
C6-H6B···Br4	0.99	3.05	3.962(5)	153.4
C7-H7B···Br4 ⁴	0.99	3.30	3.913(4)	121.6
C9-H9B···Br1	0.99	3.19	3.798(4)	121.0
C9-H9B···Br3 ³	0.99	3.22	3.818(4)	120.7
C10-H10A···Br2 ⁴	0.99	2.89	3.817(4)	156.6
C10-H10B···Br1	0.99	3.17	3.857(4)	127.7
C11-H11A···Br3 ³	0.99	3.06	3.947(4)	149.8
C11-H11B···Br2 ⁴	0.99	3.10	3.995(4)	151.0
C11-H11B···Br3 ⁴	0.99	2.88	3.505(4)	122.0
C12-H12A···Br2 ⁵	0.99	2.99	3.818(4)	142.2
C13-H13B···N2 ⁶	0.99	3.11	3.859(6)	133.4
C15-H15A···Br1	0.99	3.13	3.761(4)	123.3
C15-H15A···N2 ⁶	0.99	2.74	3.606(5)	145.9
C15-H15B···Br3 ³	0.99	2.96	3.847(4)	150.0

¹-X,1-Y,2-Z; ²-X,-1/2+Y,3/2-Z; ³-X,1-Y,1-Z; ⁴1+X,+Y,+Z; ⁵1+X,3/2-Y,-1/2+Z; ⁶-X,1/2+Y,3/2-Z

Table S3 Hydrogen bonds for 2.

D-H···A	D-H/Å	H-A/Å	D-A/Å	D-H-A/°
O4-H4C···Br2 ²	0.85	2.44	3.293(3)	178.8
O4-H4D···Br1 ³	0.85	2.44	3.287(3)	175.6
O5-H5C···Br2	0.85	2.44	3.288(3)	176.1
O5-H5D···Br1 ³	0.85	2.47	3.291(3)	163.3
C1-H1A···Br2 ⁴	0.99	3.05	3.846(4)	138.3
C1-H1A···O4 ⁵	0.99	2.8	3.709(5)	152.3
C1-H1B···Br2 ⁶	0.99	2.89	3.798(4)	153.6
C2-H2A···Br1 ⁴	0.99	2.98	3.747(4)	135
C2-H2B···Br2 ⁴	0.99	3.11	3.891(5)	136.8
C2-H2B···O5 ⁴	0.99	2.83	3.712(6)	148.8
C3-H3A···O1 ⁷	0.99	3.01	3.819(5)	139.2
C3-H3A···O3 ⁷	0.99	2.99	3.817(5)	142.3
C3-H3A···O4 ⁷	0.99	2.99	3.630(5)	123.3
C3-H3B···O4 ⁵	0.99	3.06	3.903(5)	144
C4-H4A···O5 ⁴	0.99	2.82	3.703(6)	148.9
C4-H4B···O1 ⁷	0.99	3.14	3.876(6)	132.6
C4-H4B···O4 ⁷	0.99	3.04	3.690(6)	124.6
C5-H5A···O5 ²	0.99	2.88	3.523(5)	123.1
C5-H5B···O3 ⁷	0.99	2.84	3.714(5)	147.1
C7-H7A···O4 ⁵	0.99	2.79	3.703(5)	154.2
C7-H7B···O3 ⁷	0.99	2.61	3.536(5)	155.4
C8-H8A···Br1 ⁷	0.99	3.15	3.877(4)	131

¹-X,1/2+Y,1/2-Z; ²1+X,1/2-Y,1/2+Z; ³-X,-1/2+Y,1/2-Z; ⁴-X,1-Y,1-Z; ⁵1-X,1/2+Y,3/2-Z;⁶1+X,+Y,1+Z; ⁷1-X,1-Y,1-Z

2. Supporting figures

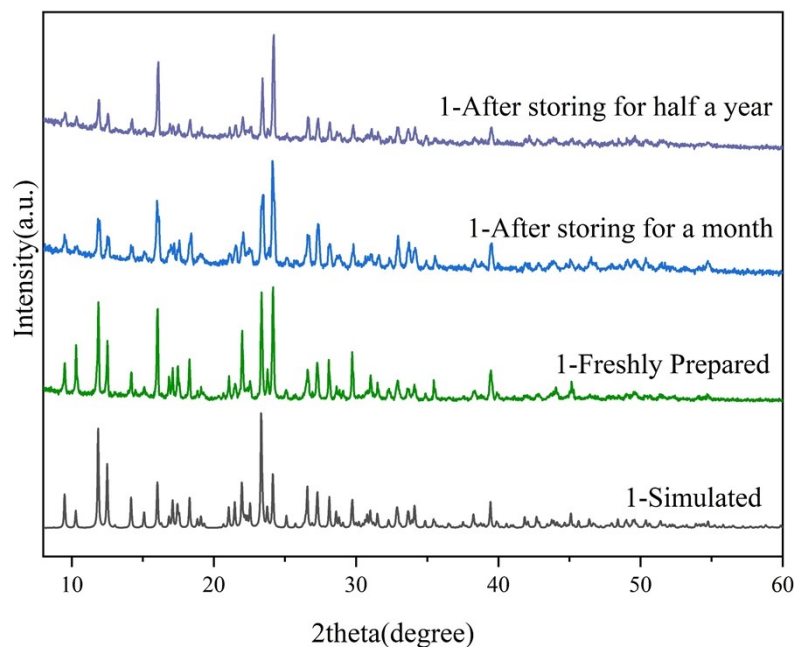


Fig. S1 Experimental and simulated PXRD patterns of 1.

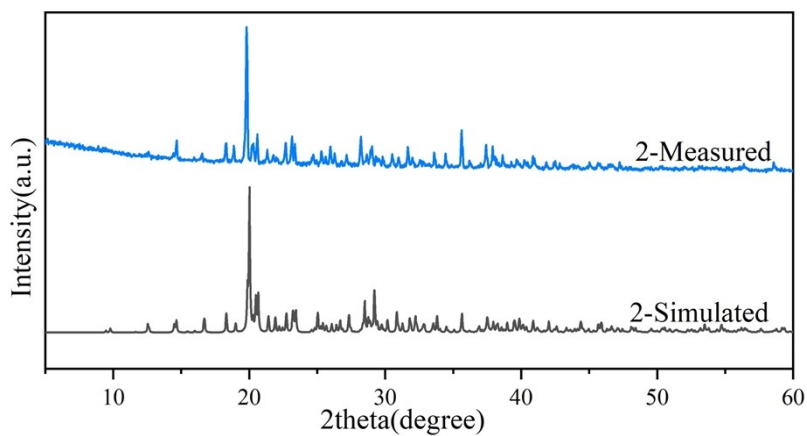


Fig. S2 Experimental and simulated PXRD patterns of 2.

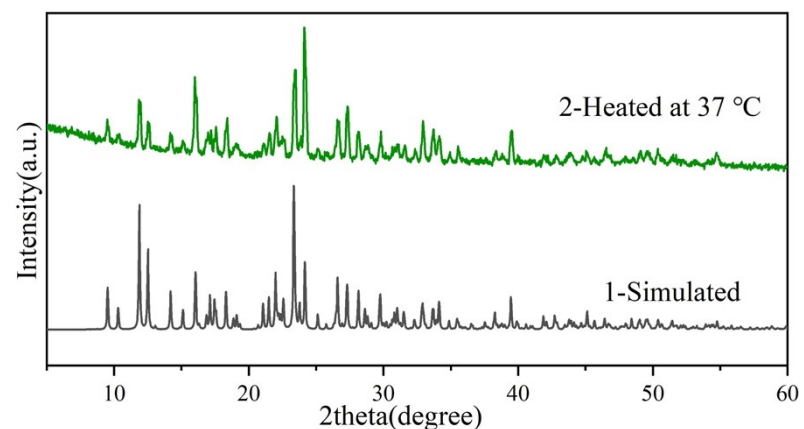


Fig. S3 Experimental PXRD pattern of 2 after heating it at 37 °C and simulated PXRD pattern of 1.

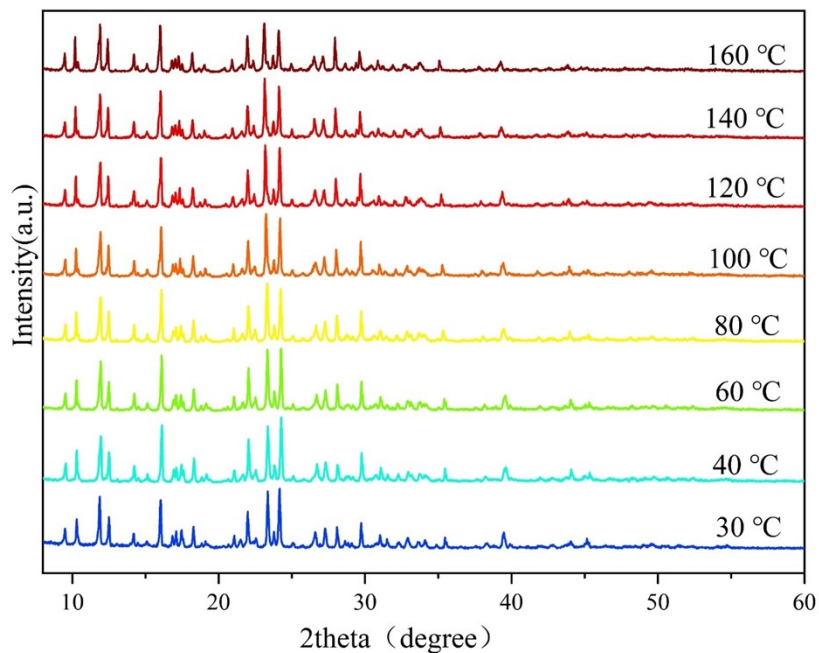


Fig. S4 Temperature-dependent PXRD data of **1**.

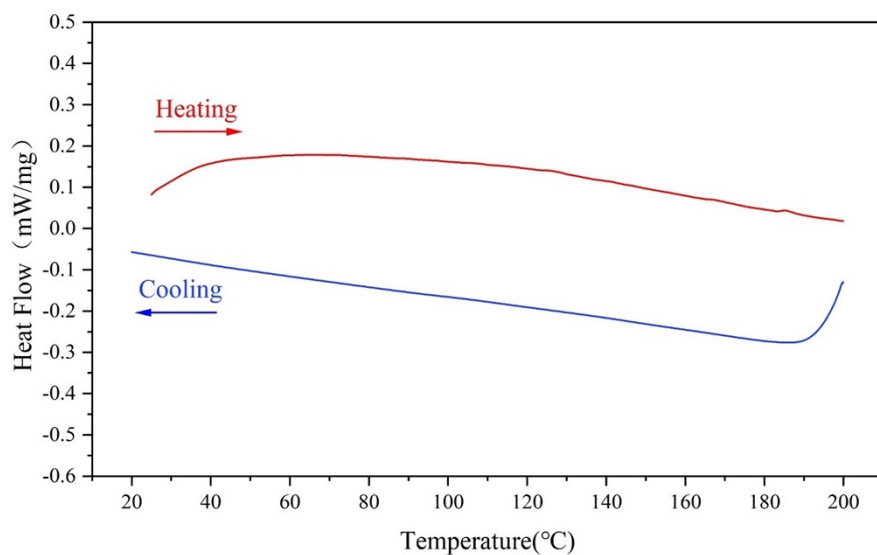


Fig. S5 DSC curves of **1** powder measured in the temperature range of 25–200 °C.

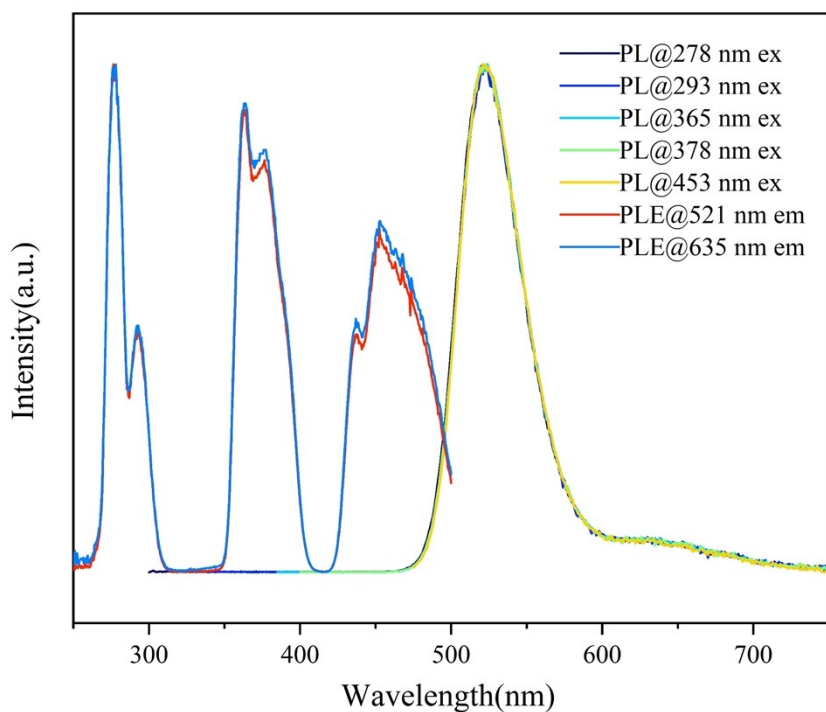


Fig. S6 Normalized Excitation-wavelength dependent PL spectra Emission-wavelength-dependent PLE spectra of **1**.

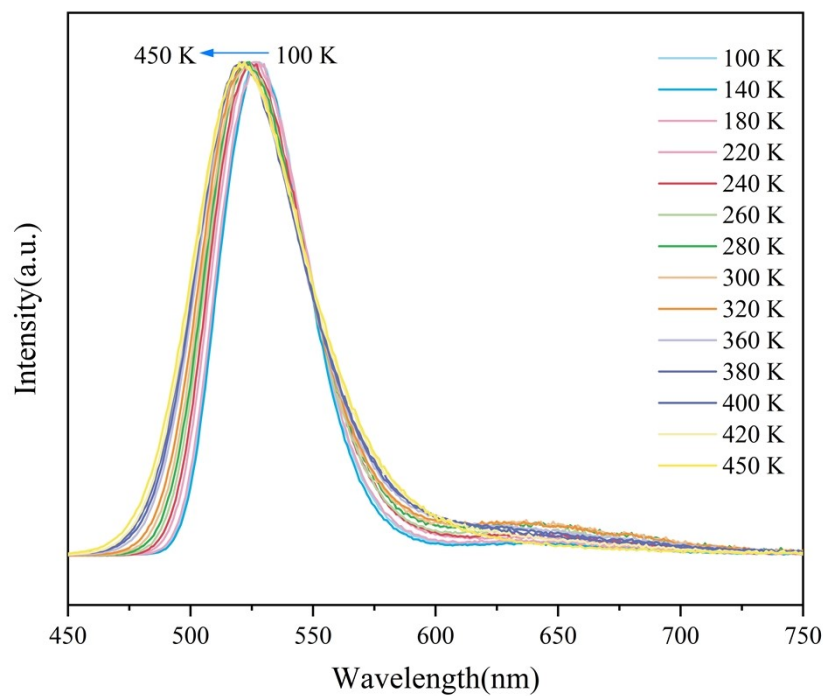


Fig. S7 Normalized temperature-dependent PLE Spectrum of **1**.

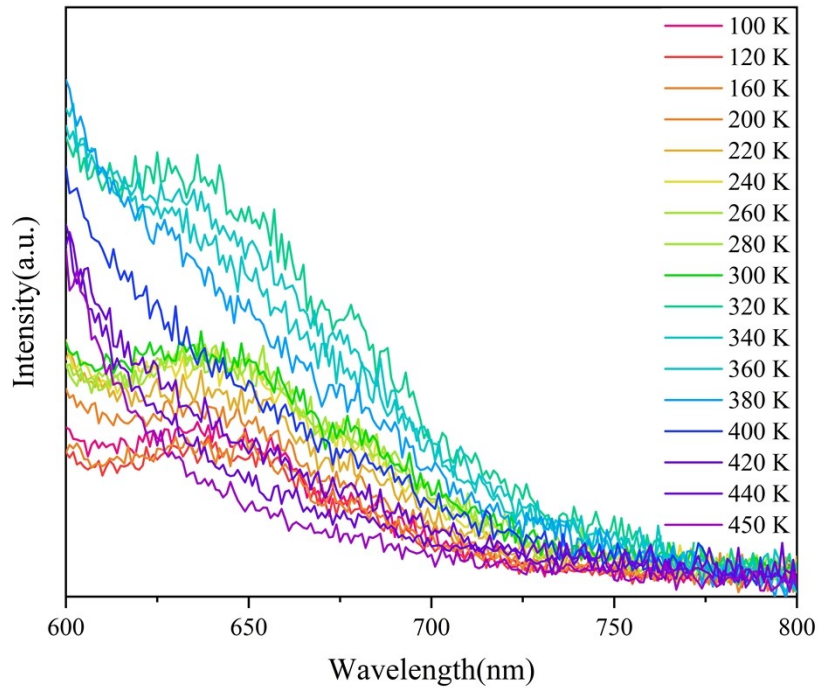


Fig. S8 Temperature-dependent PLE Spectrum of peak 2 in **1**.

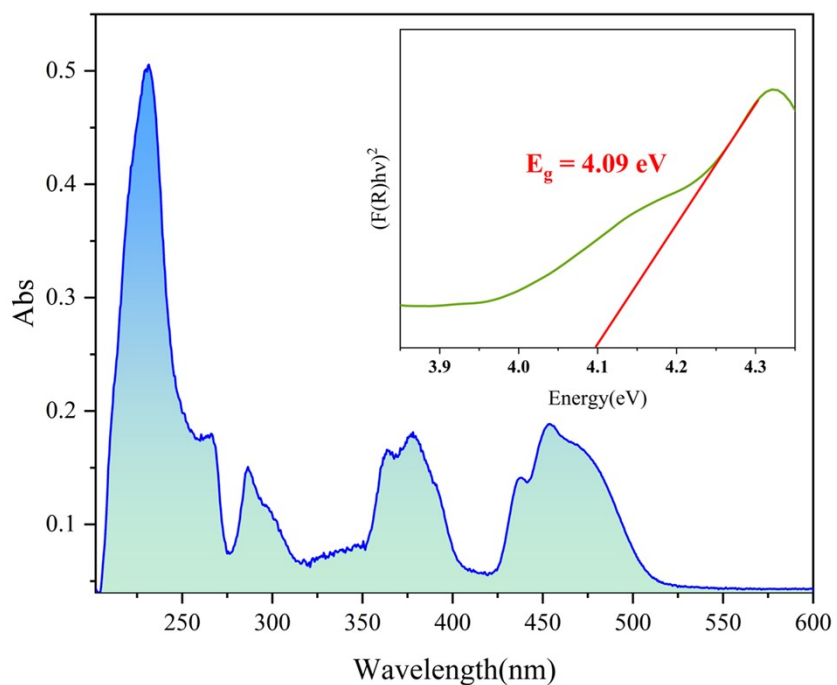


Fig. S9 UV-Vis absorption spectrum and corresponding Tauc plots of **1**.

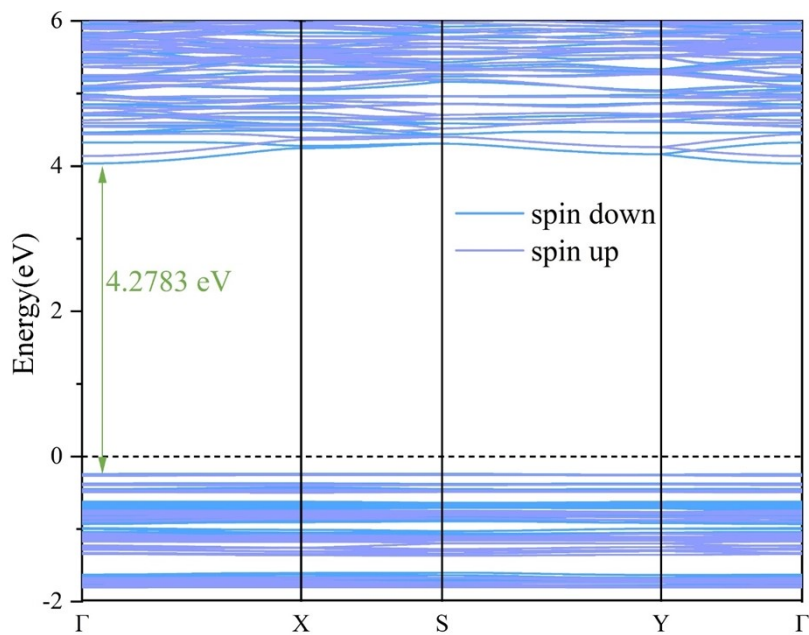


Fig. S10 DFT Calculated band structure of **1**.

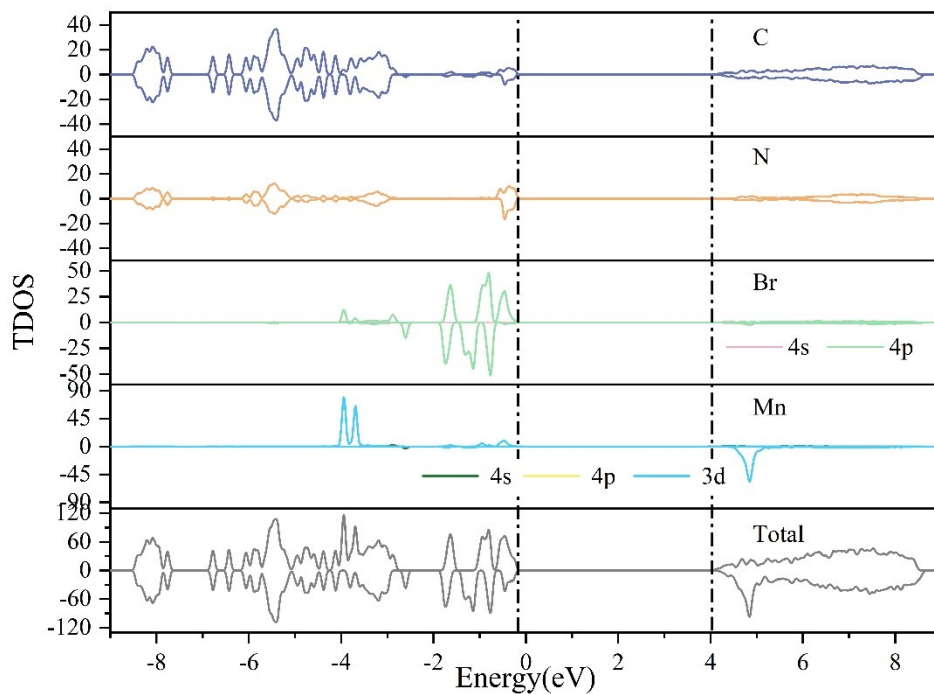


Fig. S11 The total and orbital projection of partial density of states of **1**.

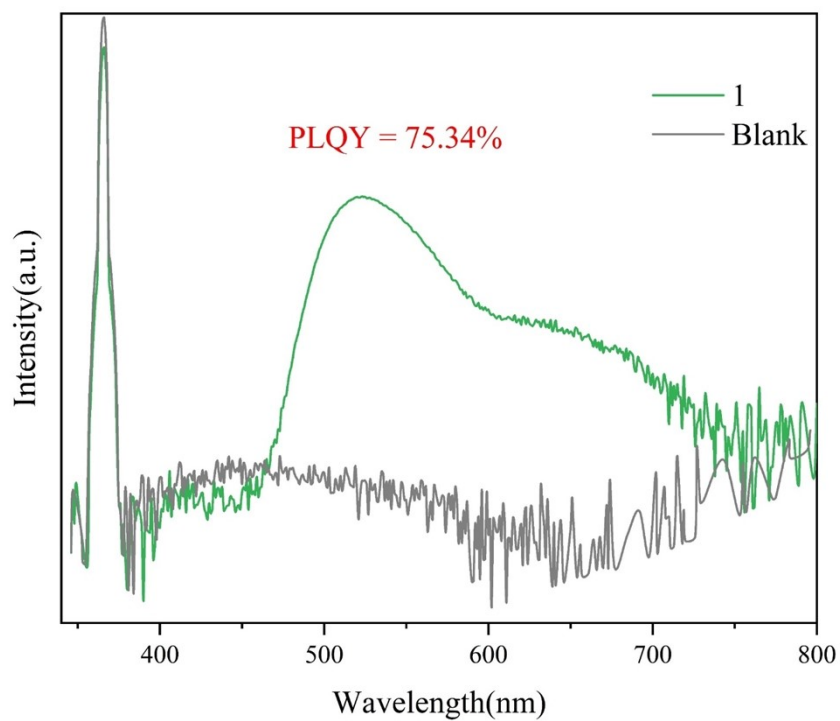


Fig. S12 Absolute PLQY of **1** at room temperature.

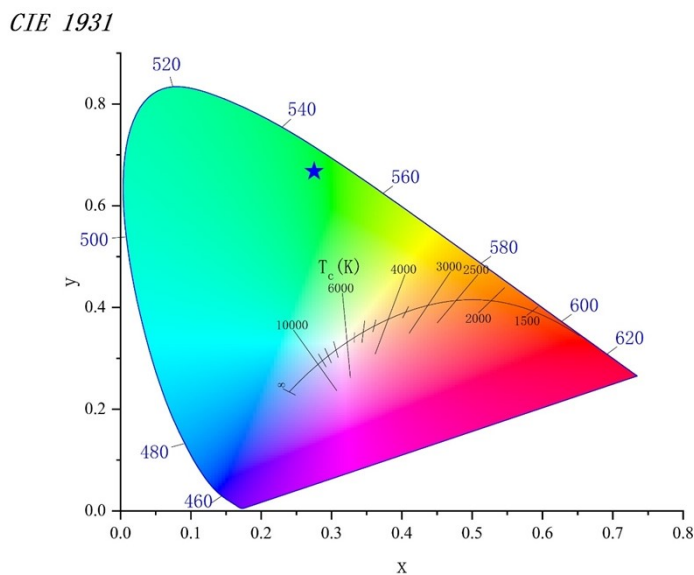


Fig. S13 CIE diagram of **1** at room temperature.

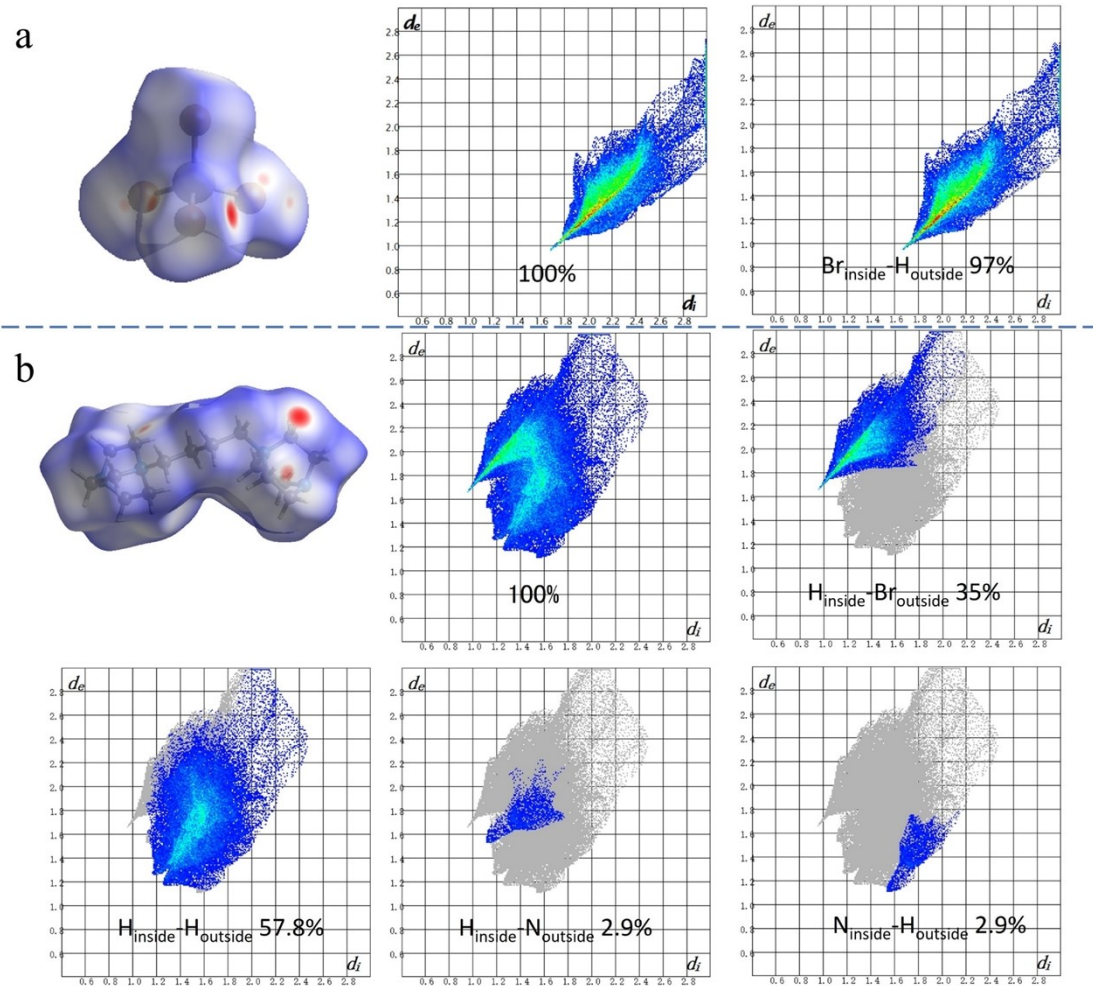


Fig. S14 The Hirshfeld d_{norm} surfaces and 2D fingerprint plots of (a) $[MnBr_4]^{2-}$ tetrahedron and (b) BBD cation in **1**.

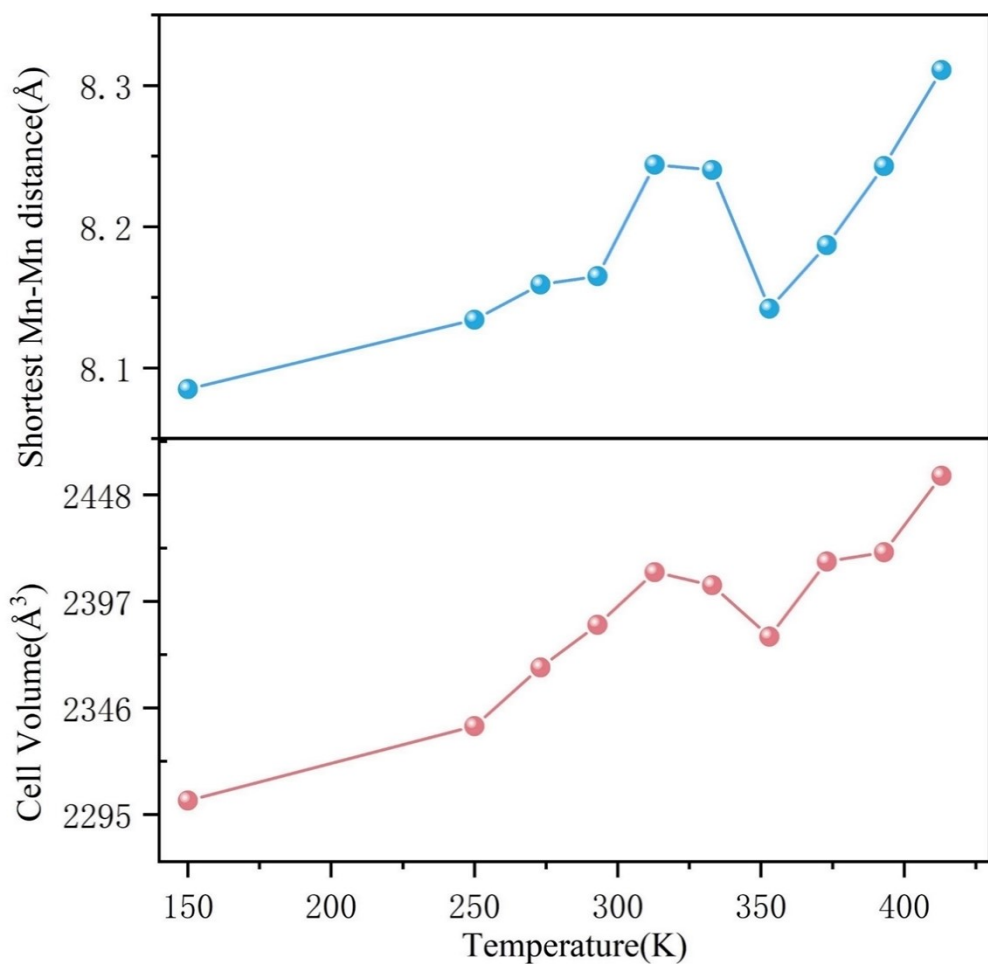


Fig. S15 Temperature-dependent shortest Mn-Mn distance and cell volume of **1** from SCXRD data.

CIE 1931

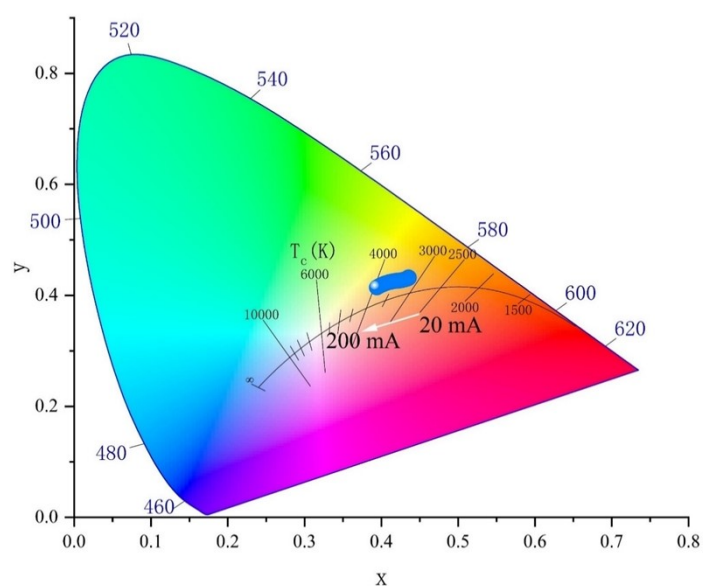


Fig. S16 CIE chromaticity coordinates changes under the driving currents range from 20 to 200 mA of the WLED device.

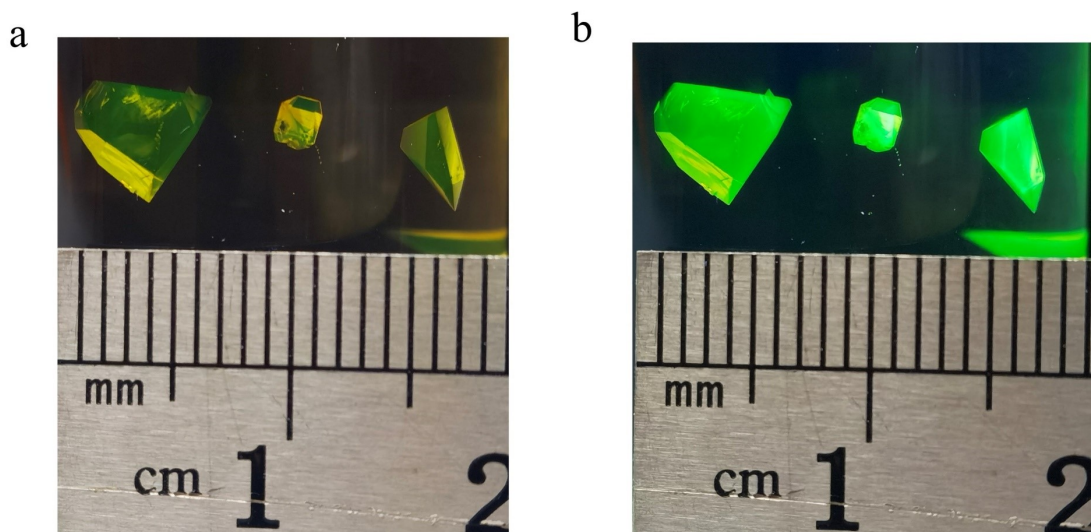


Fig. S17 Photographs of bulk single crystal of **1**. (a) under visible light. (b) under UV light.

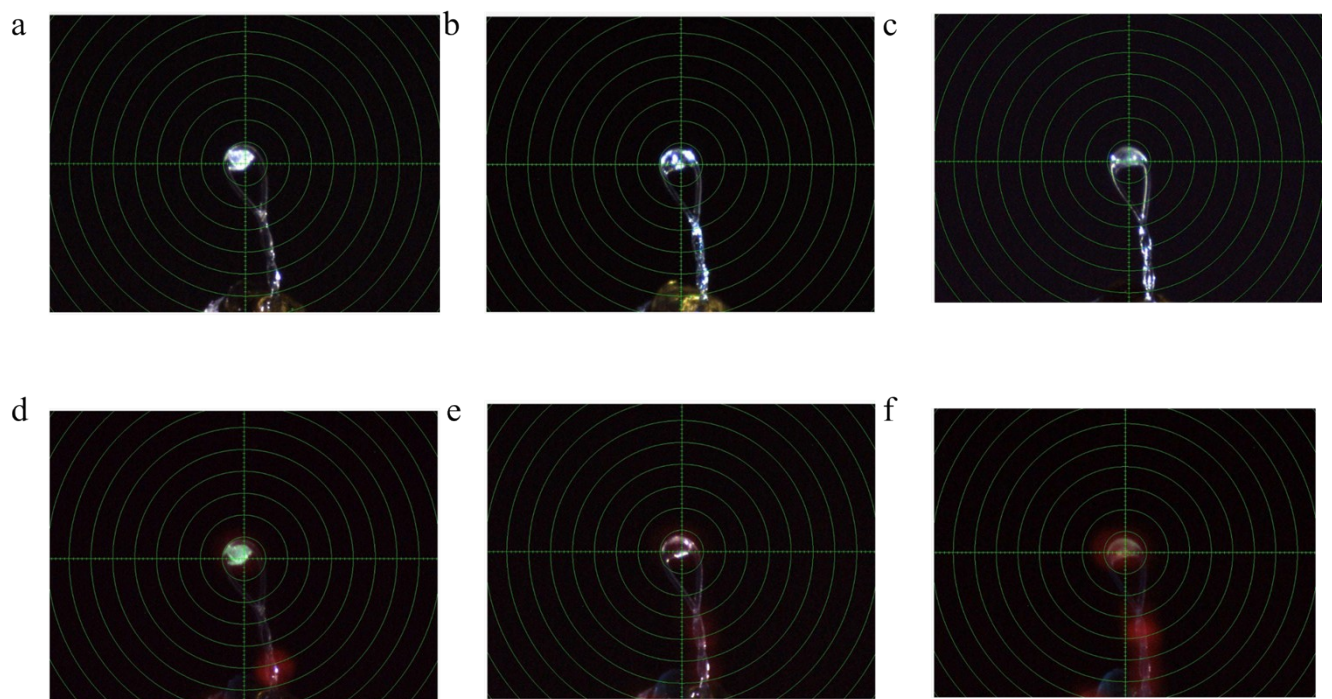


Fig. S18 *In-situ* single crystal images in the process: a transition from phase **1** to phase **2**, finally return to phase **1**. (a)-(c) under visible light. (b)-(f) under UV light.



Fig. S19 *In-situ* single crystal unit cell parameters of a transition from phase **2** to phase **1**.